ACS Macro Letters

Letter

pubs.acs.org/macroletters

Band-to-Nonband Transition into Unique Poly(ε-caprolactone) Crystals by Modulating the Interplay of Diffusion and Growth

Yiguo Li,[†] Haiying Huang,[†] Tianbai He,*[,†] and Zongbao Wang*[,‡]

[†]State Key Laboratory of Polymer Physics and Chemistry, Changchun Institute of Applied Chemistry, Chinese Academy of Sciences, Graduate School of the Chinese Academy of Sciences, Changchun 130022, P. R. China

[‡]Ningbo Key Laboratory of Polymer Materials, Ningbo Institute of Material Technology and Engineering, Chinese Academy of Sciences, Ningbo, 315201, P. R. China

Supporting Information

ABSTRACT: Previously, by modulating the interplay of chain diffusion and crystal growth rate in evaporating solution-cast poly(ε-caprolactone) (PCL) thin films, discrete banded crystals were obtained when diffusion and growth are competitive. In this study, we further investigated the effect of diffusion and growth, here mainly the growth rate on the crystallization of PCL. We found that there is a threshold (or range of) growth rate above which the banding cannot develop, and thus a band-to-nonband transition leads to the emergence of a novel crystal pattern. Accompanied by the band-to-nonband transition, the lamellar orientation also changes from flat-on to mainly tilted or even edge-on. The result reveals the significant impact of the diffusion and growth, especially the growth rate on the crystal construction and then the crystal morphology.

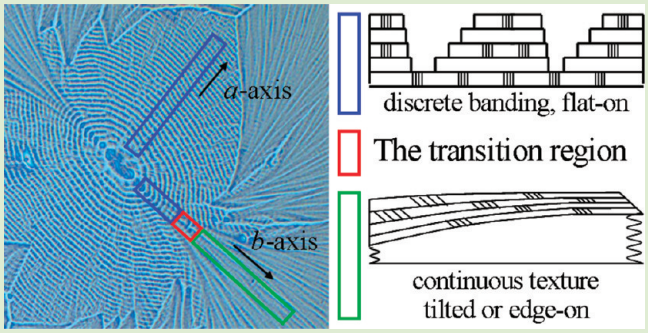

Studies of the crystallization and morphology in polymer thin films are of particular interest and importance due to their fascinating features and significant impact on material properties.[1−4] It has been shown that the same crystallizable species can exhibit fiber-like, labyrinthine, dendritic, seaweed, compact, and faceted patterns, depending on crystallization conditions.[3] Despite the extensive number and variety of experiments, understanding and controlling the generation of diverse crystal patterns have been rather elusive.[2−7] Herein, we will focus on exploring the formation of a novel crystal pattern.

Recently, we obtained unusual banded crystals with a discrete structure in solution-cast poly(ε-caprolactone) (PCL) thin films by controlling solvent extraction and thus modulating the interplay of chain diffusion and crystal growth.[8,9] These banded crystals formed upon slow solvent evaporation when chain diffusion and crystal growth are competitive. Similar ringed patterns were also observed in isotactic polystyrene (iPS) and poly(bisphenol A hexane ether) (BA-C6) melt-crystallized thin films.[10−12] Unlike the classical banded spherulites result from the periodic twisting of lamellar crystals along the radial direction,[13] the fancy banded pattern is derived from the inability of the diffusive process to keep up with the radial growth.[8−12] It has suggested that the band periodicity is proportional to diffusion length l, which can be represented by $l = D/V$, the ratio of diffusivity to the growth velocity V. It is, therefore, reasonable to expect that, once the l decreases to a threshold value below which the discrete banded crystals are not accessible, concomitantly a band-to-nonband transition should take place.

To substantiate such an idea, therefore, we will focus on investigating the band-to-nonband transition by further tuning the interplay of chain diffusion and crystal growth. As a result, a novel crystal pattern could be obtained. In drying solution-cast thin films, the faster the solvent extraction rate is employed, the time scale allowed for the diffusion and growth is shorter, so that as the evaporation rate increases, a smaller and smaller l should induce the disappearance of the discrete banding. PCL was chosen due to its good crystallizing ability. We obtained a band-to-nonband transition induced novel PCL crystal pattern by controlling solvent withdrawing of solution-cast thin films with a gradually increased rate. With the transition of lamellar packing from discrete to continuous, the lamellar orientation also changes from flat-on to mainly tilted or even edge-on. It shows that solely having a critical growth rate is sufficient to trigger these changes of lamellar packing and orientation that results in the emergence of the unique crystal pattern.

A PCL with a weight and number average molecular weight of 14 000 and 10 000 g mol^{-1} was purchased from Aldrich Chemicals and used as received. The material was dissolved in toluene at a concentration of 5 mg mL^{-1}. A portion of 10 μL of solution was dropped onto the cleaned silicon wafer placed on

Received: April 27, 2012
Accepted: May 18, 2012
Published: May 24, 2012

   dx.doi.org/10.1021/mz300212r | ACS Macro Lett. 2012, 1, 718−722

a stage lodged inside a weighing bottle with a radius and height of 2.0 cm and 2.5 cm. After casting, the bottle was covered with a piece of glass immediately. The solution film was then dried at room conditions (temperature, 18−22 °C and relative humidity, RH, 18−30%). As the solvent extracts, the crystallization of the PCL takes place. With drying the solution film thickness reduces gradually, and the decrease in the center is faster than that in the edge, in which the rapidest extraction inducing an outward flow carries liquid to replenish the evaporating solvent.[14] The thickness of the resulting thin films lies between 200 and 300 nm, and the thickness in the center is lower than that in the edge, but this thickness difference does not alter the nature of the formed crystal pattern.

The resulting thin film was first investigated by an optical microscope (OM; Carl Zeiss A2m microscope). Figure 1 gives

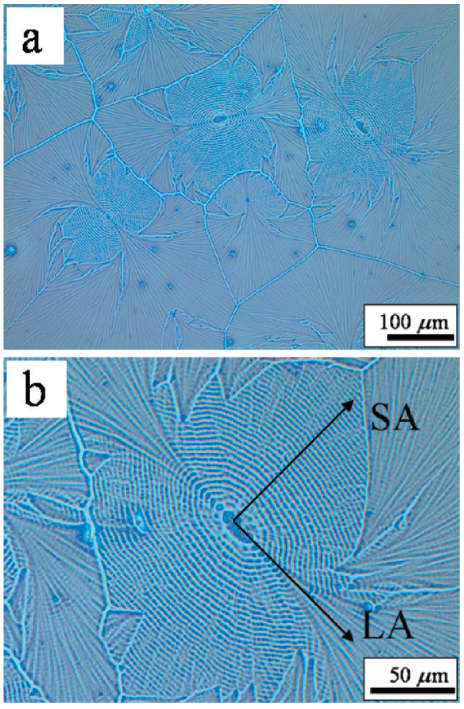

Figure 1. OM photographs exhibiting the unique morphological features of the PCL crystals.

the typical OM photographs of the PCL crystals in the thin film dried at a temperature and RH of 20 °C and 25%, respectively. The crystals show a novel morphology that consists of the central region with a banded pattern and the around zone with radiating fibrous texture. The radiating texture starts to evolve along the opposite long axis (LA) and then wraps around the central banding that leads to the appearance of the peculiar pattern. The LA and short axis (SA) are defined by the truncated lozenge shaped core, which are clearly discernible in Figure 2f and 3c. In the LA direction as the axial distance increases, the banding becomes poorly developed and eventually disappears, while in the SA direction the band spacing decreases continuously from ∼5 to ∼2 μm. Furthermore, in the LA direction the banding number varies in different crystals, which determines the size of the banded region. In other words, the band-to-nonband transition occurs in different axial lengths. This behavior is better illustrated in the enlarged images given in Figure S1 of the Supporting Information. In conclusion, a band-to-nonband transition takes place in the LA direction. A similar crystal pattern was also observed when poly(ethylene succinate) crystallized in molten thin films, but no banding was observed in the LA direction, and thus no band-to-nonband transition occurred.[15]

To further uncover the transition in the intriguing pattern, AFM (atomic force microscopy, PICOSCAN SPM, Molecular Imaging Inc., now Agilent 5500AFM/SPM System (Agilent Technologies)) was applied to characterize the detailed architecture. As shown in Figure 2a, the major characters of

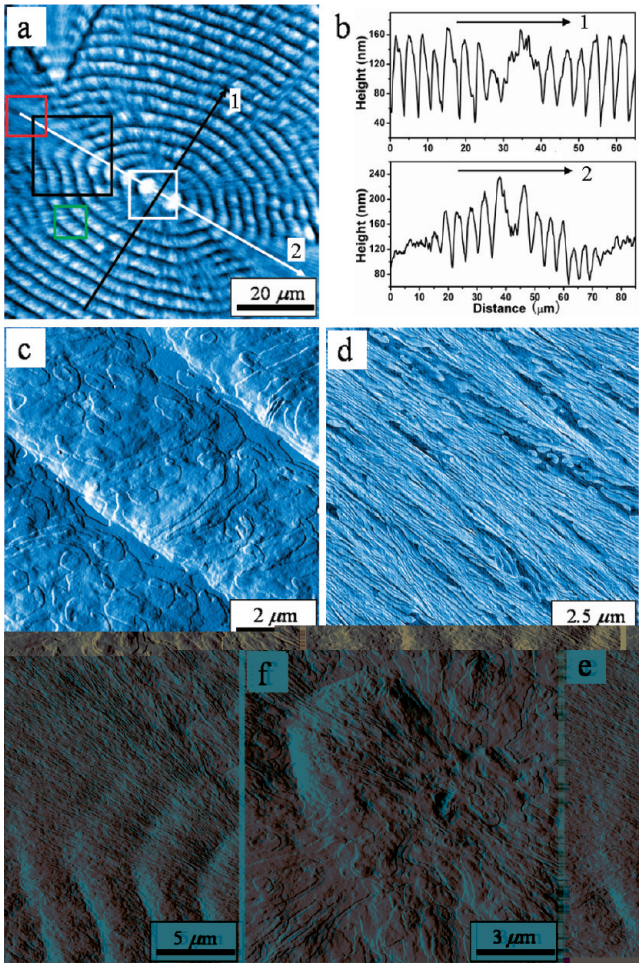

Figure 2. AFM images displaying the construction of the novel morphology. (a) Overall height picture, (b) cross-sectional height profiles along the lines added in part a, amplitude images of (c) banded pattern, (d) fibrous texture, (e) transition zone, and (f) central truncated lozenge-shaped structure. Zones c, d, e, and f are indicated by green, red, black, and white squares in part a, respectively.

the exciting pattern are again apparent. Figure 2b reveals that in the banded region the thickness varies rhythmically that leads to the appearance of the banded feature, and that an almost uniform thickness yields from the around fibrous texture. Figure 2c exhibits that the banded pattern is composed of discrete stacks of flat-on lamellae, and Figure 2d displays that the fibrous texture consists of continuous packing of predominantly tilted or even edge-on lamellae. Clearly, the morphological features of the banded pattern are identical with that of the PCL discrete banded crystals.[8] It is now fully convinced that a band-to-nonband transition indeed occurs in the LA direction, which drives the generation of the unique crystal pattern. Specifically, when the lamellar packing changes

dx.doi.org/10.1021/mz300212r | ACS Macro Lett. 2012, 1, 718−722

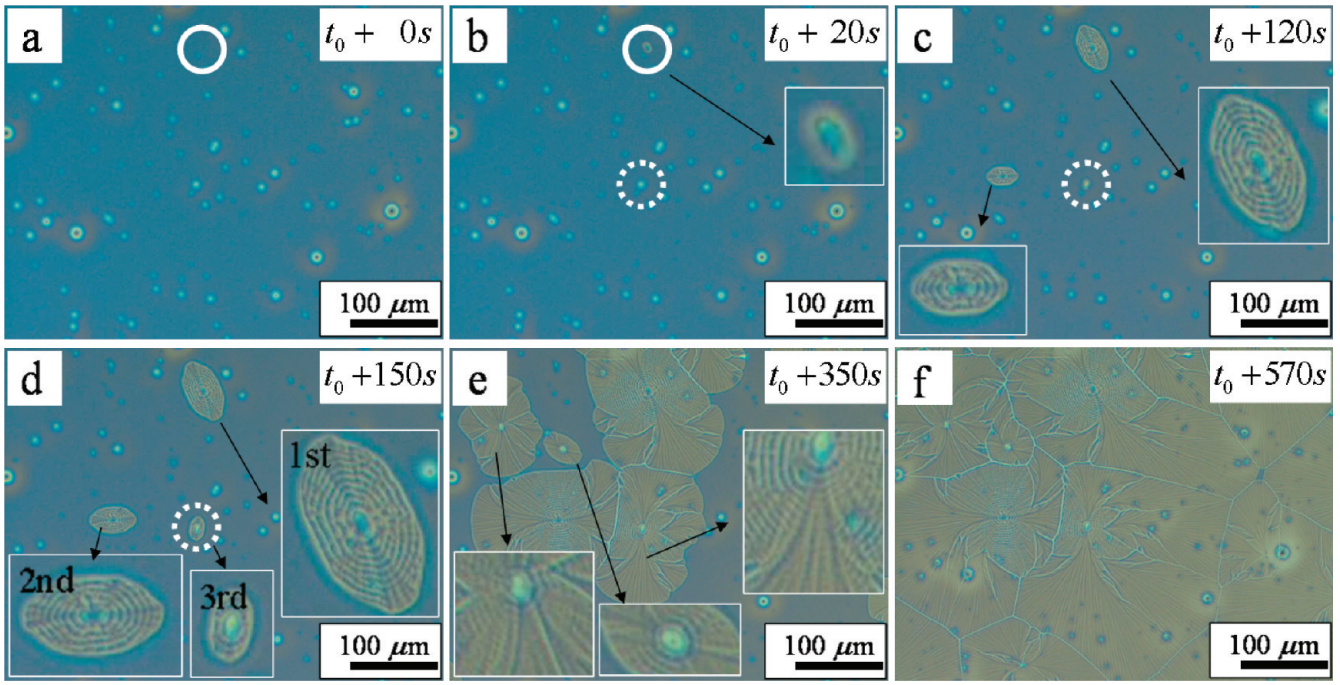

Figure 3. (a) In situ OM micrographs depicting the detailed growth process of the PCL crystals. Here, t_0 = 480 s. The growth curves for the first, second, and third crystals are labeled as 1, 4, and 5 in Figure 4. Insets here in b, c–d, and e are enlarged 6, 3, and 4 times respectively relative to the original pictures.

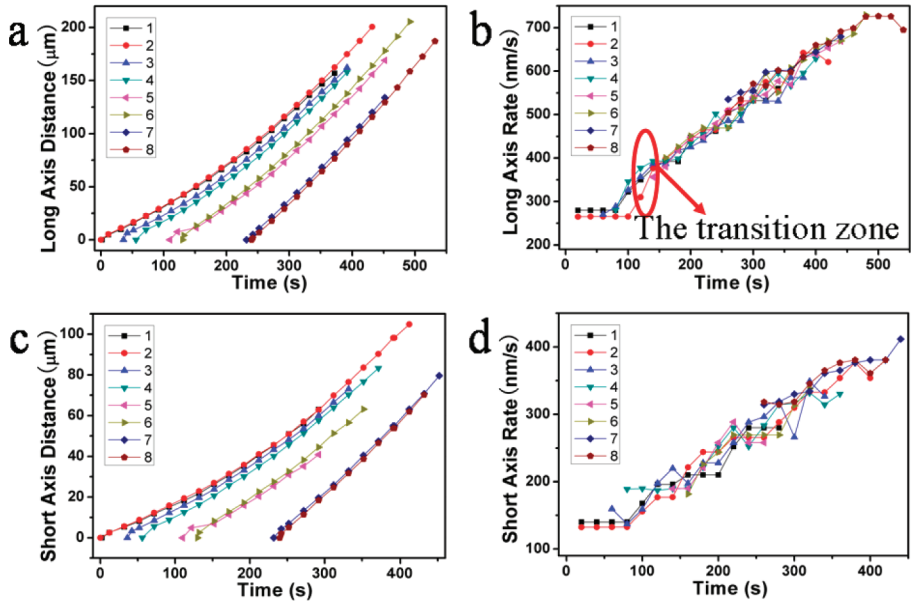

Figure 4. Temporal changes of axial distance and rate with time for different crystals in LA (a, b) and SA (c, d) directions. The data confirm a gradual increased axial growth rate resulting in the band-to-nonband transition along LA and continued decrease of band spacing along SA. Here t = 0 s corresponds to the time point for the appearance of the first crystal. The in situ development process is available in Video S1 in the Supporting Information, and the crystals and axial directions are labeled in Figure S2.

from discrete banding to a continuous radiating texture, the lamellar orientation also shifts from flat-on to mainly tilted or even edge-on (Figure 2e). It has shown that the orientation of lamellae depends on crystallization conditions such as film thickness, temperature, and polymer–substrate interaction.[4−6,16] It is not obvious that these differences exist in the same film, so the origin for the changes in lamellar packing and orientation remains puzzling.

Figure 2f displays that the hexagonal core is also comprised of stacks of lamellae with an almost flat-on orientation. This point is different from that of most spherulites in which the center exhibits a sheaf-like structure.[7] But this hexagonal core resembles PCL single crystals formed from solution and lamellar crystals obtained at 54 °C in thin films with a thickness range from 200 to 30 nm.[17,18] In those crystals the SA and LA correspond to the crystallographic *a*- and *b*-axes, and the hexagonal shape is limited by two {100} and four {110} sectors.

dx.doi.org/10.1021/mz300212r | *ACS Macro Lett.* 2012, 1, 718–722

Due to the similar construction, it is reasonable that in these crystals the SA and LA also represent the *a*- and *b*-axes.

To obtain insight into the morphology transition and pattern formation, a continuous shooting mode OM with a time interval of 2 s was performed to follow the whole drying process of the solution thin film. The nucleation was clearly spotted to start within 8 min, and the crystal growth finished within 10 min. The whole process is available in Video S1 of the Supporting Information, and Figure 3 gives a series of OM pictures depicting the evolvement of the crystals. Except for some foreign particles, no crystal was formed during the first 8 min (Figure 3a). Another 20 s later, a small crystal appeared (Figure 3b). As the growth proceeded, crystals with a truncated lozenge shape and periodic banding were discernible (Figure 3c). Subsequent growth resulted in poor development and then the disappearance of the banding along the LA direction. Instead, the fibrous texture developed (Figure 3d,e). Finally, the rapid extended fibrous texture along LA suppressed and warped around the slower developed banding in the SA direction, so that the novel crystals resulted (Figure 3e,f). As mentioned above, the band-to-nonband transition occurred at a changed axial distance in different crystals. Specifically, the banding vanished nearly simultaneously in different crystals between 120 and 150 s (Figure 3c and d). From then on, the new formed crystals no longer exhibit any banding in LA (Figure 3e). That is, after a fixed time point (or time interval) the banding does not form at all in the LA direction. Hence, it is the nucleation time rather than the axial length that determines the band-to-nonband transition. The earlier the crystal nucleated, the more the banding evolved in LA, and thus the larger the banded region observed.

To further analyze the structural generation, quantitative measurement of the growth rate is more informative. For comparison and to eliminate occasionality, we chose eight crystals nucleated at different times, and each two appeared at the almost same time. It can be seen that the growth along both LA and SA directions displays nonlinear features (Figure 4a and c), which is quite different from the constant rate of the spherulitic crystals formed from the melt. Clearly, the growth of SA is much slower than that of LA. The time dependence of growth rate is clearly illustrated in Figure 4b and d. For the first formed crystals, initially the growth rate is nearly invariant, but it slowly increases as the growth progresses. While for the latter crystals the growth rate always increases with time. Furthermore, the curves are superposable with respect to time irrespective of different crystals. This means that the growth rate depends on the evolution time rather than the axial growth distance of individual crystal. The behavior is in accord with that the banding diminishes simultaneously in all crystals. A comparison of Figure 3 with Figure 4 further indicates the important role of the growth rate having on the band-to-nonband transition and the band spacing. During the early stage the invariant rate corresponds to the constant spacing in both LA and SA directions. Then a continued increase of growth rate drives the band-to-nonband transition along LA and the decrease of band spacing along SA. The change from band to fibrous texture takes place when the growth rate lies between 300 and 400 nm s^{-1}. Due to the lower growth rate (less than 400 nm s^{-1}) the banding always develops in the SA direction. Hence, the increase in growth rate should be responsible for the band-to-nonband and orientation transition and then the generation of the peculiar crystals. The variant axial direction growth rate was also observed in poly[(*R*)-3-hydroxyvalerate], which likewise led to the occurrence of a fancy crystal pattern.[19]

During the drying process, one encounters two different processes: solvent evaporation and solute crystallization. The solute crystallization is derived from solution supersaturation induced by the solvent extraction. Once nucleation occurred, the evaporation rate determines the time for chain diffusion and crystal growth and consequently the growth rate. At the early stage, the rapid extraction makes a balance between the solvent withdrawn from solution and that escaped outside, and thus a constant partial pressure causes the nearly steady evaporation. But, as the process progresses, the continued reduction of surface area and concomitantly the gradual decrease in solvent pressure accelerate the evaporation. Hence, the growth rate increases with the drying time.

Crystal growth in thin films is associated with molecular diffusion.[2] The growth pattern can be explained by the diffusion length l, which is found to be strongly dependent on the diffusion coefficient D and the growth rate V.[3,10,20] This effect can be expressed as $l \propto D/V$. D mainly relies on the molecular weight, temperature, and solution concentration. Herein, the former two are invariant. The rapid evaporation and crystal growth indicate that the rather small change of supersaturated concentration, so the change of D is rather slight and can be neglected. The approximate invariant of D can also be specified by the fact that a ca. 2.5 times increase in growth rate drives a nearly equal decrease of band spacing in the SA direction. Hence, the major variant is the V. Due to the gradual rather than abrupt increase in V and the constant existence of the concentration difference between the crystal and the concentrated solution, there are weaker and weaker bands along the LA direction. Hence, as the V increases, the l continuously reduces, and thus the banding becomes poorly developed and eventually diminishes, which gives rises to the transition of the morphological feature from discrete banding to a continuous texture. The similar reduction of l is also responsible for the periodicity decrease in SA. Likewise, the increase in V leads to the transition of lamellar orientation from mainly flat-on to random, resembling that of temperature dependence of lamellar orientation in melt.[6,16] It has been established that the lamellar width is also proportional to D/V.[21] This effect is evident from Figure S3 of the Supporting Information that the lamellae in SA are somewhat wider than those in LA. It can be concluded here that there is a threshold V and then l below which the discrete banding no longer develops and concomitantly the band-to-nonband transition takes place.

In summary, by modulating the interplay of chain diffusion and growth crystal, a band-to-nonband transition is observed above a threshold growth rate, which leads to the occurrence of a novel morphology of PCL crystals. Accompanied by this transition of lamellar packing from discrete banding to continuous texture, the lamellar orientation also changes from flat-on to mainly tilted or even edge-on. With the gradual increase of the growth rate, the band-to-nonband transition occurred in the faster evolved *b*-axis, whereas the banding with continuously reduced spacing always existed in the slower developed *a*-axis. This observation provides an excellent demonstration of the statement that the morphology of crystals is determined not only by the crystal structure itself, but by the process of that growth. The finding first richens the polymer crystal morphologies and is also envisaged to deepen the understanding of pattern formation during polymer crystallization in thin films.

dx.doi.org/10.1021/mz300212r | *ACS Macro Lett.* 2012, 1, 718−722

■ ASSOCIATED CONTENT

Supporting Information

OM images of the unique PCL crystals with different sizes of banded region, crystal numbers and axial directions corresponding to the curves of Figure 4, and an AFM image of the lamellar crystals (Figures S1−S3, pdf) and the drying process of the solution thin film followed by in situ OM (Video S1, avi). This material is available free of charge via the Internet at http://pubs.acs.org.

■ AUTHOR INFORMATION

Corresponding Author

*E-mail: tbhe@ciac.jl.cn (T.H.); wangzb@nimte.ac.cn (Z.W.).

Notes

The authors declare no competing financial interest.

■ ACKNOWLEDGMENTS

This work was supported by the National Science Foundation of China (21074135 and 21004073).

■ REFERENCES

(1) Frank, C. W.; Rao, V.; Despotopoulou, M. M.; Pease, R. F. W.; Hinsberg, W. D.; Miller, R. D.; Rabolt, J. F. *Science* **1996**, *273*, 912−915.
(2) Ramanathan, M.; Darling, S. B. *Prog. Polym. Sci.* **2011**, *36*, 793−812.
(3) Zhang, G.; Zhai, X.; Ma, Z.; Jin, L.; Zheng, P.; Wang, W.; Cheng, S. Z. D.; Lotz, B. *ACS Macro Lett.* **2012**, *1*, 217−221.
(4) Liu, Y. X.; Chen, E. Q. *Coord. Chem. Rev.* **2010**, *254*, 1011−1037.
(5) Yang, J. P.; Liao, Q.; Zhou, J. J.; Jiang, X.; Wang, X. H.; Zhang, Y.; Jiang, S. D.; Yan, S. K.; Li, L. *Macromolecules* **2011**, *44*, 3511−3516.
(6) Wang, Y.; Chan, C. M.; Ng, K. M.; Li, L. *Macromolecules* **2008**, *41*, 2548−2553.
(7) Chan, C. M.; Li, L. *Adv. Polym. Sci.* **2005**, *188*, 1−41.
(8) Wang, Z. B.; Hu, Z. J.; Chen, Y. Z.; Gong, Y. M.; Huang, H. Y.; He, T. B. *Macromolecules* **2007**, *40*, 4381−4385.
(9) Wang, Z. B.; Alfonso, G. C.; Hu, Z. J.; Zhang, J. D.; He, T. B. *Macromolecules* **2008**, *41*, 7584−7595.
(10) Duan, Y. X.; Jiang, Y.; Jiang, S. D.; Li, L.; Yan, S. K.; Schultz, J. M. *Macromolecules* **2004**, *37*, 9283−9286.
(11) Duan, Y. X.; Zhang, Y.; Yan, S. K.; Schultz, J. A. *Polymer* **2005**, *46*, 9015−9021.
(12) Wang, Y.; Chan, C. M.; Li, L.; Ng, K. M. *Langmuir* **2006**, *22*, 7384−7390.
(13) Lotz, B.; Cheng, S. Z. D. *Polymer* **2005**, *46*, 577−610.
(14) Deegan, R. D.; Bakajin, O.; Dupont, T. F.; Huber, G.; Nagel, S. R.; Witten, T. A. *Nature* **1997**, *389*, 827−829.
(15) Kawashima, K.; Kawano, R.; Miyagi, T.; Umemoto, S.; Okui, N. *J. Macromol. Sci., Part B* **2003**, *42*, 889−899.
(16) Wang, Y.; Rafailovich, M.; Sokolov, J.; Gersappe, D.; Araki, T.; Zou, Y.; Kilcoyne, A. D. L.; Ade, H.; Marom, G.; Lustiger, A. *Phys. Rev. Lett.* **2006**, *96*, 028303.
(17) Iwata, T.; Doi, Y. *Polym. Int.* **2002**, *51*, 852−858.
(18) Mareau, V. H.; Prud'homme, R. E. *Macromolecules* **2005**, *38*, 398−408.
(19) Ye, H. M.; Xu, J.; Guo, B. H. *Macromolecules* **2009**, *42*, 694−701.
(20) Keith, H. D.; Padden, F. J. *J. Appl. Phys.* **1964**, *35*, 1270−1285.
(21) Reiter, G.; Sommer, J. U. *Phys. Rev. Lett.* **1998**, *80*, 3771−3774.